Model-Based Control of a 3-DOF Parallel Robot Based on Identified Relevant Parameters

Miguel Díaz-Rodríguez, Angel Valera, Vicente Mata, and Marina Valles

***Abstract*—This paper presents in detail how to model, identify, and control a 3-DOF prismatics-revolute-spherical parallel manipulator in terms of relevant parameters. A reduced model based on a set of relevant parameters is obtained following a novel approach that considers a simplified dynamic model with a physically feasible set of parameters. The proposed control system is compared with the response of a model-based control that considers the complete identification of the rigid-body dynamic parameters, friction at joints, and the inertia of the actuators. The control systems are implemented on a virtual and an actual prototype. The results show that the control scheme based on the reduced model improves the trajectory tracking precision when comparing with the control scheme based on the complete set of dynamic parameters. Moreover, the reduced model shows a significant reduction in the computational burden, allowing real-time control.**

***Index Terms*—Dynamic parameter identification, model-based control, parallel robots, robot control.**

I. Introduction

PARALLEL manipulators (PMs) are mechanisms where a moving platform is connected to a base through several kinematic chains (legs) [1]. Over the last two decades PMs have been a very active research topic, mainly because they work at higher speed and with greater stiffness and positioning accuracy when compare to serial robots. The main concern is that the complexity of the dynamic model of a PM is greater than it is in a serial robot.

In recent years, industrial applications [2] and medical robots [3] which require high stiffness, high accuracy, and fast motion have been designed based on PM structures. These robots needs the implementation of an advanced control system to achieve fast and accurate motion [4]; therefore, several control systems have been proposed in [5]–[8] and [9].

Advanced control systems require the computation of a dynamic model. Due to the complexity of a PM model, simplified dynamic modeling approaches are introduced in [10], [11], and [12]. In [10], the simplified model is obtained by neglecting the leg masses and inertias of a class of PM, but this assumption cannot be generalized for other PMs. In [11], the robot structure is designed so that some terms of the dynamic model could be simplified. However, this approach is not applicable to a robot which is already built. In [12], a factor that distributes the mass of the robot's legs between the moving platform and the prismatic joint of a 3-prismatics-revolute-cilindrical PM is proposed; thus, leg dynamics are simplified from the dynamic model. Since the mass distribution factors are not constant when considering different trajectories, this approach is impractical for advanced control systems.

On the other hand, advanced control systems require the identification of the model parameters which can be obtained by fitting a dynamic model to measurements. The rigid body dynamic model of a PM can be written linear with respect to the dynamic parameters, thus linear regression techniques are suitable for dynamic parameter identification [13]–[17]. However, the identification model is ill-conditioned due to the structure of a PM. Moreover, when noise is present in the measurements, identification leads to poorly identified parameters [18]. Thus, these parameters need to be simplified to obtain a reliable identification model. Two approaches are used as a reduction criterion: the relative standard deviation [19] and the contribution of the identified parameters to the system dynamics [20]. The model is reduced until a specific threshold value is satisfied.

This paper presents in detail how to model, identify, and control a PM considering a simplified model (reduced model) with physically feasible parameters. These two aspects have not been considered previously for model-based control of PMs. Physical feasibility is an important aspect for improving model-based control [21]. A 3-DOF prismatic-revolute-spherical PM (3-PRS, where P stands for the actuated joint) is presented as a case study. The parameters of control systems are obtained through numerical simulations and experiments Two model-based controls are used: 1) a reduced model and 2) for comparison purposes, a complete model.

The results show that the control system based on the reduced model behaves better than when the complete set of dynamic parameters is considered. In addition, a study of the computational burden of the reduced model and the complete model is presented. Results show that the reduced model presents a significant reduction in the computational burden, allowing real-time control.

This paper is organized as follows. Section II presents the methodology for the dynamic parameter identification of a PM; the computational burden of the reduced model and the complete

Manuscript received May 2, 2012; accepted July 25, 2012. Date of publication August 27, 2012; date of current version December 11, 2013. Recommended by Technical Editor S. K. Saha. This work was supported in part by the Spanish Government under Grant DPI2010-20814-C02-01 (IDEMOV) and in part by the Consejo de Desarrollo Científico, Humanístico y Tecnológico de la Universidad de Los Andes (CDCHT-ULA) under Grant I-1286-11-02-B.

M. Díaz-Rodríguez is with the Departamento de Tecnología y Diseño, Facultad de Ingeniería, Universidad de los Andes, Mérida 5101, Venezuela (e-mail: dmiguel@ula.ve).

A. Valera and M. Valles are with the Departamento de Ingeniería de Sistemas y Automática, Universidad Politécnica de Valencia, Valencia 46022, Spain (e-mail: giuprog@isa.upv.es; mvalles@isa.upv.es).

V. Mata is with the Centro de Investigación de Tecnología de Vehículos, Universidad Politécnica de Valencia, Valencia 46033, Spain (e-mail: vmata@mcm.upv.es).

Digital Object Identifier 10.1109/TMECH.2012.2212716

model is studied. Section III develops the model-based control of a 3-PRS PM. Section IV shows the results for the control system applied to a virtual prototype. Section V shows the results for the control system applied to an actual PM. Finally, Section VI presents the conclusions.

II. Modeling and Identification of a PM in Terms of Relevant Parameters

The equation of motion for a mechanical system is obtained as in [4] by considering a noncentroidal coordinate frame such that

$$\mathbf{K}_{rb} \cdot \vec{\Phi}_{rb} = \vec{Q}_{\text{ext}} + \mathbf{A}_q^T \cdot \vec{\lambda}. \tag{1}$$

In (1), $\mathbf{K}_{rb}(\vec{q}, \dot{\vec{q}}, \ddot{\vec{q}})$ depends on the generalized coordinates and their time derivatives. The vector $\vec{Q}_{\text{ext}}$ contains the external generalized forces, $\mathbf{A}_q$ is the Jacobian matrix, and $\vec{\lambda}$ is the vector of Lagrange multipliers. The vector $\vec{\Phi}_{rb}$ contains the inertia parameters of the ith link, $[m_i, mx_i, my_i, mz_i, Ixx_i, Ixy_i, Ixz_i, Iyy_i, Iyz_i, Izz_i]^T$.

When performing a dynamic parameter identification, a widely accepted model for friction at joints is a linear one in parameters [22]. Then, the dynamic model considering rigid body dynamics and a linear friction model at the joints can be written as follows:

$$[\,\mathbf{K}_{rb} \quad \mathbf{K}_{fr}\,] \cdot \begin{bmatrix} \vec{\Phi}_{rb} \\ \vec{\Phi}_{fr} \end{bmatrix} = \vec{Q}_{\text{ext}} + \mathbf{A}_q^T \cdot \vec{\lambda} \tag{2}$$

where matrix $\mathbf{K}_{fr}(\dot{\vec{q}})$ considers a velocity-dependent viscous and Coulomb friction model, $\vec{\Phi}_{fr} = [\ldots Fc_j \; Fv_j \ldots]$ contains the friction parameters.

Since no experimental information is available with respect to the internal forces $\mathbf{A}_q^T(\vec{\lambda})$, they are eliminated from (2) using the coordinate partitioning method [23], which leads to

$$\left(\mathbf{K^i} - \mathbf{X}^T \cdot \mathbf{K^s}\right) \cdot \vec{\Phi} = \vec{\tau}^i - \mathbf{X}^T \cdot \vec{\tau}^s. \tag{3}$$

In (3), $\mathbf{K} = [\,\mathbf{K}_{rb} \quad \mathbf{K}_{fr}\,]$ apply for the generalized coordinates, velocities, and accelerations for the ith pose of the robot, $\vec{\Phi} = [\,\vec{\Phi}_{rb} \quad \vec{\Phi}_{fr}\,]^T$, $\mathbf{X} = (\mathbf{A}_q^s)^{-1} \cdot \mathbf{A}_q^s$, and $\vec{\tau}$ is the vector of the generalized forces. Subscripts s and i stand for the dependent and independent generalized coordinates.

The dimension of $\vec{\tau}^i$ is to a large extent lower than that of the vector $\vec{\Phi}$. Thus, different sets of measurements $(\vec{q}, \dot{\vec{q}}, \ddot{\vec{q}})$ and $\vec{\tau}^i$ are taken along a prescribed trajectory which leads to the following equation:

$$\mathbf{W} \cdot \vec{\Phi} = \vec{\tau}. \tag{4}$$

Equation (4) is an overdetermined linear system that could be solved by least squares methods, but for a general mechanical system this linear system cannot be solved because the columns of $\mathbf{W}$ are not independent ones. This is because some of the inertial parameters have no effect on the system's dynamic behavior, and some parameters affect this behavior in linear combinations. Different approaches are considered in [24] to obtain the set of base parameters (parameters that contribute in linear combinations), but even those parameters are difficult to be identified. Some of them make few or even insignificant contributions to the system's dynamic behavior, leading to an ill-conditioned identification model. In order to avoid ill-conditioning of $\mathbf{W}$, a simplified set of parameters can be used such that

$$\mathbf{W}^* \cdot \vec{\Phi}^* = \vec{\tau} \tag{5}$$

where * stands for a model expressed in terms of the base parameters or a simplified set of parameters.

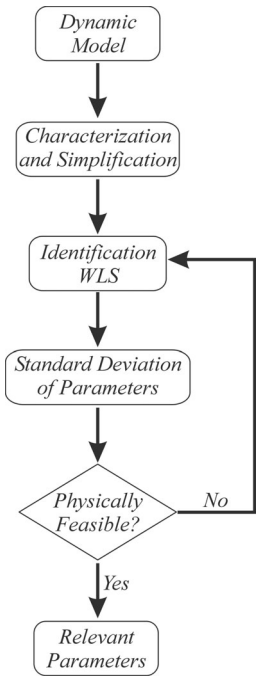

Fig. 1. Flowchart of the process to obtain a set of relevant parameters.

Usually, the simplification process considers the link geometries and the symmetries of the mechanical system. However, it is worth noting that until [25], the physical feasibility of the set of identified parameters had not been introduced as a key issue in the simplification process for modeling a PM. This aspect as mentioned before is a critical one to ensure the stability of some model-based control schemes [21]. The objective of this paper is to develop a model-based control system based on a set of relevant parameters. The methodology to obtain the identification model in terms of the relevant parameters is summarized in Fig. 1. First, the dynamic model is established in term of the base parameters. Then, the link geometries and the symmetry of the mechanical system are taking into account to simplify (5). Afterward, the dynamic parameters are identified by using WLS. The parameters are sorted by considering their standard deviation, and the physical feasibility conditions are verified. If the set of parameters is not feasible, the parameter with maximum standard deviation is eliminated. Thereafter, reduction continues until the set of parameters corresponding to a reduced model is physically feasible.

III. Dynamic-Based Control System

A. Dynamic Model for Model-Based Control

Model-based control requires writing the equation of motion as follows [26]:

$$\mathbf{M}(\vec{q},\vec{\Phi})\ddot{\vec{q}} + \vec{C}(\vec{q},\dot{\vec{q}},\vec{\Phi}) + \vec{G}(\vec{q},\vec{\Phi}) = \vec{\tau}. \tag{6}$$

In (6), $\mathbf{M}$ stands for the mass matrix, $\vec{C}$ is the vector of centrifugal and Coriolis terms, and $\vec{G}$ is the vector of the gravitational forces. Each term of (6) needs to be written in terms of the identified dynamic parameters (relevant or base parameters). This is achieved in this paper inspired by classical algorithms [27].

The gravitational term depends on the generalized coordinates. Thus, the vector $\vec{G}$ is calculated by zeroing velocities and accelerations in (5). This can be expressed as:

$$\mathbf{W}^*(\vec{q},\dot{\vec{q}}=0,\ddot{\vec{q}}=0)\cdot\Phi^* = \vec{G}(\vec{q},\vec{\Phi}). \tag{7}$$

The columns of $\mathbf{M}$ is calculated as follows:

$$\mathbf{W}^*(\vec{q},\dot{\vec{q}}=0,\vec{u}_k)\cdot\Phi^* = \mathbf{D}_k(\vec{q}) \tag{8}$$

where $\mathbf{D}_k$ is the kth column of the mass matrix and $\vec{u}_k = [0\ \ldots\ 1\ \ldots]^T$. Due to constrains, $\mathbf{D}_k$ contains dependent and independent generalized coordinates, thus the generalized dependent accelerations are obtained with respect to the generalized independent acceleration as follows:

$$\ddot{\vec{q}}_s = \left(\mathbf{A}_q^s\right)^{-1}\cdot\vec{b} - \mathbf{X}\cdot\ddot{\vec{q}}_i. \tag{9}$$

In (9), $\vec{b}$ is the bias vector which depends on the velocity and generalized coordinates. The dependent accelerations are eliminated by using (9):

$$\mathbf{D}^i\cdot\ddot{\vec{q}}_i + \mathbf{D}^s\cdot((\mathbf{A}_q^s)^{-1}\cdot\vec{b} - \mathbf{X}\cdot\ddot{\vec{q}}_i). \tag{10}$$

From (10), it can be seen that the term $\mathbf{D}^s\cdot(\mathbf{A}_q^s)^{-1}\cdot\vec{b}$ corresponds to centrifugal and Coriolis forces. This term is part of to vector $\vec{C}$. Finally, $\mathbf{M}$ is obtained as follows:

$$\mathbf{M}(\vec{q},\vec{\Phi}) = \mathbf{D}^i - \mathbf{D}^s\cdot\mathbf{X}. \tag{11}$$

Vector $\vec{C}$ is obtained by zeroing the generalized acceleration in (5) minus the gravity vector ($\vec{G}$), and adding the centrifugal Coriolis force from (10), thus obtaining the following equation:

$$\mathbf{W}^*(\vec{q},\dot{\vec{q}},\ddot{\vec{q}}=0)\cdot\Phi^* - \vec{G}(\vec{q},\vec{\Phi}) + \mathbf{D}^s\cdot(\mathbf{A}_q^s)^{-1}\cdot\vec{b} = \vec{C}(\vec{q},\dot{\vec{q}},\vec{\Phi}). \tag{12}$$

B. Dynamic Model for a 3-PRS PM

Model-based control systems are developed for the 3-PRS PM depicted in Fig. 2. The PM consists of three legs connecting the moving platform to the base. Each leg contains: 1) a motor driving a ball screw, 2) a slider, and 3) a connecting rod. The lower part of the ball screws are perpendicularly joined to the base platform. The position of the ball screws at the base is an equilateral triangle configuration. The ball screw transforms the rotational movement of the motor into linear motion. The prismatic joint (P) is assumed to be between the sliders and the corresponding ball screw. The connecting rod is joined to the upper part of the ball screw by a revolution joint (R). The moving platform is joined to the connecting rod through spherical joints (S).

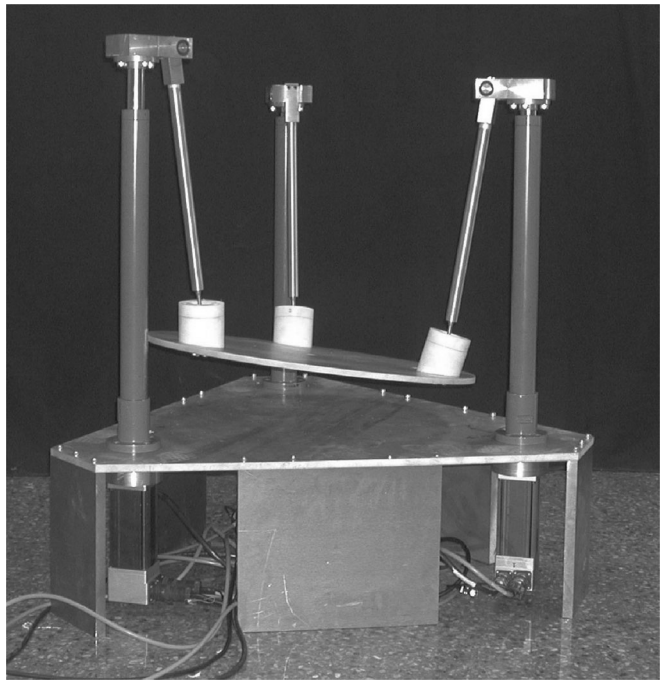

Fig. 2. 3-PRS PM.

The base parameters model was obtained by applying (1) to (4). This model is called the complete model (Model 1); only the rigid body parameters are presented in Table I.

As has been previously mentioned, the objective of this paper is to implement a set of relevant parameters in a model-based control system. The model in terms of relevant parameters is a reduced model (Model 2) and consists of the rigid body parameters 11, 17, and 18 in Table I.

Table II contains the number of operations for calculating each term of the dynamic model. The number of operations for Model 2 is lower than those in Model 1. Moreover, based on the several simulations and experiments that were performed, see Section IV, Model 2 can predict the system dynamics behavior without a significant loss of precision.

C. Control Scheme

A passivity-based control system is proposed and implemented on the 3-PRS PM. This approach solves the robot control problem by exploiting the robot system's physical structure, specifically its passivity property. Despite there being different passivity-based controllers, the control system presented in [28] is implemented. The design philosophy of this controller is to reshape the system's natural energy in such a way that the tracking control objective is achieved for a serial robot. Here, the approach is extended for developing controllers for PMs which have strong dynamic coupling. One of the differences between serial and PMs is that, in the former all joints are active, while in the latter there are passive joints. The passive coordinates have to be determined within the control loop, they are found by

TABLE I
BASE PARAMETER OF THE 3-PRS PM, SI UNITS

$\vec{\Phi}$	Base Parameter	$\vec{\Phi}$	Base Parameter
1	$Izz_2 - l_r^2 \cdot \sum_{i=1}^{2} m_i$	11	$my_3 - \sin(2\pi/3)\, l_m \cdot \sum_{i=1}^{5} m_i$
2	$mx_2 + l_r \cdot \sum_{i=1}^{2} m_i$	12	mz_3
3	my_2	13	$Izz_5 - l_r^2 \cdot \sum_{i=4}^{5} m_i$
4	$Ixx_3 - (\sin(2\pi/3))\, l_m)^2 \cdot \sum_{i=1}^{5} m_i$	14	$mx_5 - l_r \cdot \sum_{i=4}^{5} m_i$
5	$Ixy_3 + \cos(2\pi/3)\sin(2\pi/3)\, l_m^2 \cdot \sum_{i=1}^{5} m_i$	15	my_5
6	Ixz_3	16	$Izz_7 + l_r^2 \cdot \sum_{i=1}^{5} m_i$
7	$Iyy_3 - (\cos(2\pi/3)\, l_m)^2 \cdot \sum_{i=1}^{3} m_i + (\sin(2\pi/3)\, l_m) \cdot \sum_{i=4}^{5} m_i$	17	$\sum_{i=1}^{7} m_i$
8	Iyz_3	18	$mx_7 + l_r \cdot \sum_{i=6}^{7} m_i$
9	$Izz_3 - l_r^2 \cdot \sum_{i=1}^{3} m_i$	18	my_7
10	$mx_3 - \cos(2\pi/3)\, l_m \cdot \sum_{i=1}^{5} m_i$ $l_m \cdot \sum_{i=4}^{5} m_i$		

TABLE II
NUMBER OF OPERATIONS FOR COMPUTING THE DYNAMIC MODEL

	Model 1		Model 2	
	$+/-$	$\times/\div$	$+/-$	$\times/\div$
$\mathbf{M}$	639	838	46	140
$\vec{C}$	1247	2989	59	222
$\vec{G}$	91	197	31	76
$\mathbf{M}+\vec{C}+\vec{G}$	1974	4024	136	438

solving the forward dynamic problem through the Newton–Raphson method. In this control law, in addition to the nonlinear dynamic (inertial, Coriolis, and gravity) terms, a PD term is added to the control input as follows:

$$\vec{\tau}_c = \mathbf{M}(\vec{q},\vec{\Phi})\ddot{\vec{q}} + \vec{C}(\vec{q},\dot{\vec{q}},\vec{\Phi}) + \vec{G}(\vec{q},\vec{\Phi}) - \mathbf{K}_p\vec{e} - \mathbf{K}_d\dot{\vec{e}}. \quad (13)$$

In (13), $\mathbf{K}_p$ and $\mathbf{K}_d$ are positive definite matrices. For tracking control purpose, it is intuitively clear that the control system should be constructed such that the strict energy minimum $(\vec{q},\dot{\vec{q}}) = (0,0)$ of the open-loop system is shifted toward $(\vec{e},\dot{\vec{e}}) = (0,0)$. This can be achieved by modifying both the kinetic and potential energy in the desired way. Fig. 3 shows a block diagram of the control strategy. The nonlinear dynamic terms of this control scheme are based on the identified parameters.

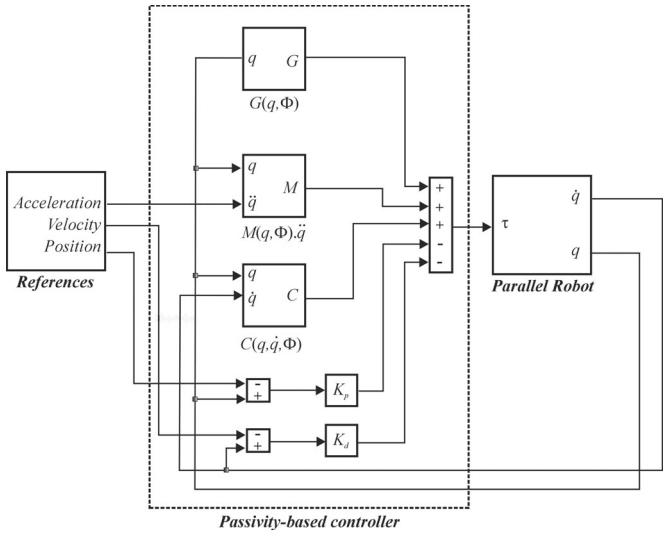

Fig. 3. Dynamic-based control scheme.

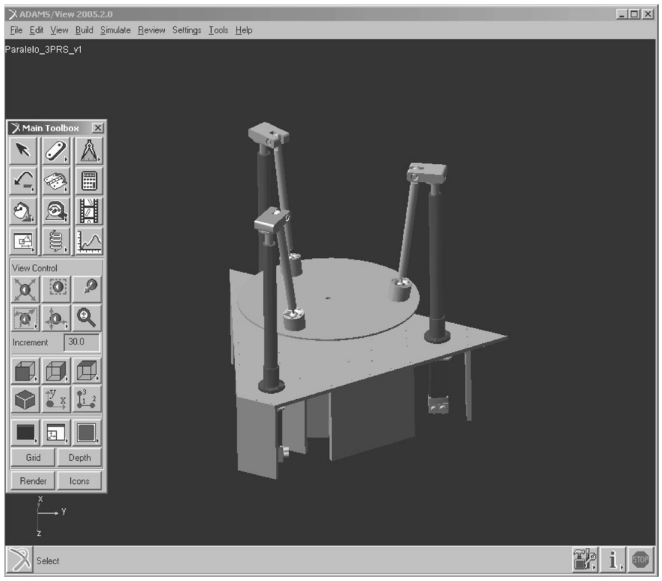

Fig. 4. Virtual prototype of the 3-PRS PM.

IV. MODEL-BASED CONTROL OF THE VIRTUAL PROTOTYPE

A. Virtual Benchmark

Three virtual prototypes were developed in MSC-ADAMS environment which is shown in Fig. 4. The kinematics and rigid body dynamic parameters are the same for all the prototypes, and they are listed in Table III (only those contributing to the robot system dynamics are listed in the table). The parameters refer to a local, gravity centered, coordinate frame. The kinematics parameter l_r is the distance between the spherical and the revolution joint. The position of the spherical joints at the platform is in equilateral configuration where l_m is the side of the triangle, and l_b is the distance between the prismatic joints located at the base.

The rotor and screw dynamics of the actuators J are included in the prototypes; J is estimated by considering the screw as a

TABLE III
KINEMATIC AND DYNAMIC PARAMETERS OF THE PROTOTYPE, SI UNITS

Kinematic Parameters	l_m	l_b	l_r				
	0.520	0.540	0.667				
Dynamic Parameter	m	Ixx	Iyy	Izz	lx	ly	lz
Body 1, 4, 6	7.46	-	-	-	-	-	-
Body 2, 5, 7	1.45	-	-	0.038	0.254	-	-
Body 3	12.56	0.468	0.468	0.929	0.210	0.121	0.489

TABLE IV
FRICTION AND ACTUATOR DYNAMICS PARAMETERS, SI UNITS

Joint	F_c	F_v	F_s	F_r	v_s	d_s	J
Prototype 1							
1	152.70	3267.45	-	-	-	-	222.75
2	118.32	2127.48	-	-	-	-	222.75
3	247.97	2120.09	-	-	-	-	222.75
Prototype 2							
1	307	1500	37.5	0.0213	1	-	222.75
2	300	1500	35.0	0.0213	1	-	222.75
3	280	1500	45.0	0.0213	1	-	222.75
Prototype 3							
1	307	1500	37.5	0.0213	1	15.27	222.75
2	300	1500	35.0	0.0213	1	11.83	222.75
3	280	1500	45.0	0.0213	1	24.79	222.75

solid cylinder. The difference among prototypes relies upon the friction model chosen at the joints. The first prototype includes a Coulomb F_c and viscous F_v friction linear model at prismatic joints. In the second one, the friction of the prismatic joints is modeled by using the following nonlinear friction model:

$$\tau_f = (F_c + (F_s - Fc) \cdot e^{|\dot{q}/vs|^{ds}}) \cdot \text{sign}(\dot{q}) + F_v \cdot \dot{q}. \quad (14)$$

An interested reader can refer to [22] for a complete understanding of this nonlinear model. The third prototype considers the aforementioned nonlinear friction model at prismatic joints and linear Coulomb friction model at revolution joints F_r. The friction and actuator dynamic parameters are listed in Table IV. Friction forces are implemented in ADAMS as externals forces located at joints. The values of the friction parameter were found by trial and error in such a way that the dynamic behavior of each prototype was as close as possible to the behavior of the actual robot.

The Fig. 5 presents a comparison between the dynamic responses of the virtual and the actual robot for one specific trajectory. Due to limitations on the length of this paper, only one of the forces exerted by the actuator of the actual and the virtual prototype is shown, but the results are similar for several trajectories. As can be seen in Fig. 5, the force values are close, so the virtual prototypes are used for designing model-based control systems. The trajectories used for estimating the friction parameters of the virtual prototypes are based on a sinusoidal function, which are described in the following section.

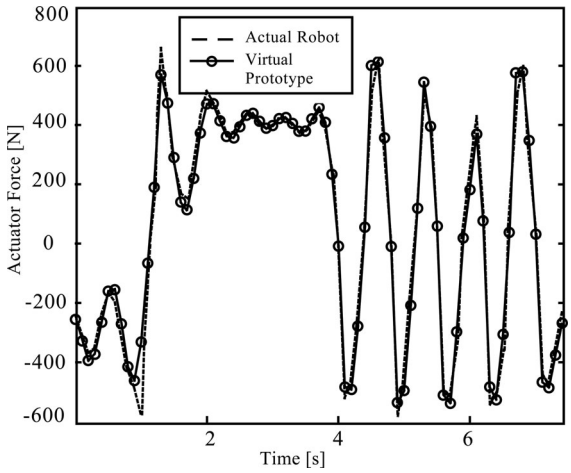

Fig. 5. Force exerted for one of the actuators.

B. Trajectories for Testing the Model-Based Control Scheme

The 3-PRS PM has one translational and two rotational DOF (1T2R). This robot is suitable when the platform requires a motion that follows two tilt angles and one translation motion of the end-effector (roll and pitch angle and vertical displacement). This type of application, for instance as a low cost driving simulator, requires the tilt angles to reach the maximum values within the reachable workspace. The following parameterization, presented in [29], is used in designing the trajectories for testing trajectories,

$$q_i(t) = q_o + \sum_{j=1}^{nH} \left[\frac{a_{ij}}{2\pi\ f\ j} \sin(2\pi\ f\ j\ t) - \frac{b_{ij}}{2\pi\ f\ j} \cos(2\pi\ f\ j\ t) \right] \quad (15)$$

where t is the time, a_{ij} and b_{ij} are the coefficients of the Fourier series that will be the variables for trajectory design, nH is the harmonic number, and f is the fundamental frequency.

Equation (15) represents a sinusoidal signal which is a common trajectory used for testing control schemes in PMs [30], [31]. An optimization process is conducted to design trajectories in which the tilt angles reach the maximum values. The optimization includes the system constraints according to the joint movements, singular configuration, and reachable workspace. Several trajectories are found; four of them are selected to perform simulations and experiments. Two of the trajectories have their linear velocity of each actuator limited to 200 mm/s; the other two trajectories are limited to 500 mm/s. An example of one of the trajectories is shown in Fig. 6. As can be seen, one of the actuators reaches its maximum stroke between 2 and 4 s, while the other two fall into their minimum values. This position corresponds to the maximum roll angle of the moving platform. Moreover, the platform reaches the minimum and maximum pitch angle between 6 and 10 s.

C. Simulations

Fig. 7 shows a flowchart of the test. First, the virtual prototype follows a test trajectory. Then, the generalized coordinates and forces are corrupted by Gaussian noise; the parameters

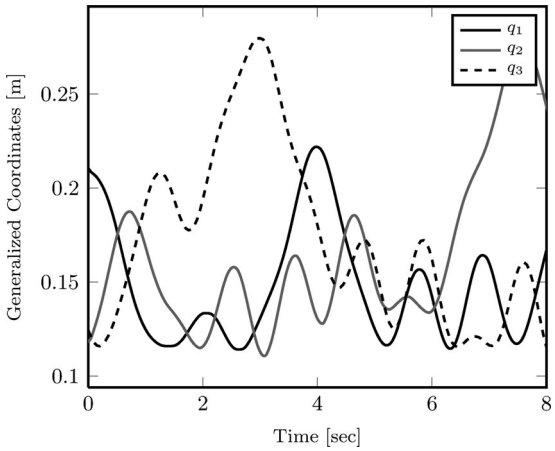

Fig. 6. Displacements of the generalized coordinates for one of the test trajectories used for simulations and experiments nH=11. Maximum speed velocity 200 mm/s.

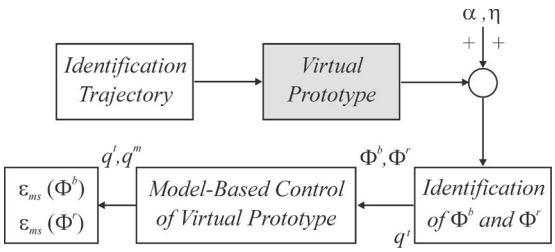

Fig. 7. Flowchart of simulations performed over the virtual prototype.

TABLE V
ROOT MEAN SQUARE FOR PROTOTYPE 1

Trajectory (ε_{RMS}) [mm]	1	2	3	4
Model 1	0.05596	0.09392	0.08558	0.12354
Model 2	0.04988	0.07933	0.07021	0.10225

for Model 1 ($\vec{\Phi}^b$) and Model 2 ($\vec{\Phi}^r$) are identified. Afterward, model-based control based on Model 1 and 2 are implemented over the prototype. The identification Model 1 considers: the rigid body parameters presented in Table I, actuator dynamics J and a Coulomb and viscous friction linear model is used for friction modeling in prismatic joints. The friction of passive joints is neglected. The identification Model 2 is obtained by reducing Model 1 until found the set of relevant parameters.

The Model 1 and the first prototype differ that in the latter the generalized coordinates and forces are corrupted by noise. In this scenario, the tracking control performance of the reduced model is tested when noise is presented in measurements. Table V shows the results for this scenario. The controller performance is measured by the root mean square (RMS) as follows:

$$\varepsilon_{\mathrm{RMS}} = \sqrt{\frac{\sum_{j=1}^{N}\sum_{i=1}^{\mathrm{DOF}}\left(q_{ij}^{m}-q_{ij}^{t}\right)^{2}}{N\cdot DOF}} \tag{16}$$

where q_{ij}^m represents the actual displacement of the actuator, q_{ij}^t the desired actuator displacement, j the sampling point of the actual trajectory for N measured data.

TABLE VI
ROOT MEAN SQUARE FOR PROTOTYPE 2

Trajectory (ε_{RMS}) [mm]	1	2	3	4
Model 1	0.05596	0.09392	0.08558	0.12354
Model 2	0.04988	0.07933	0.07021	0.10225

TABLE VII
ROOT MEAN SQUARE FOR PROTOTYPE 3

Trajectory (ε_{RMS}) [mm]	1	2	3	4
Model 1	0.06592	0.13500	0.09563	0.18938
Model 2	0.06275	0.10296	0.09075	0.13883

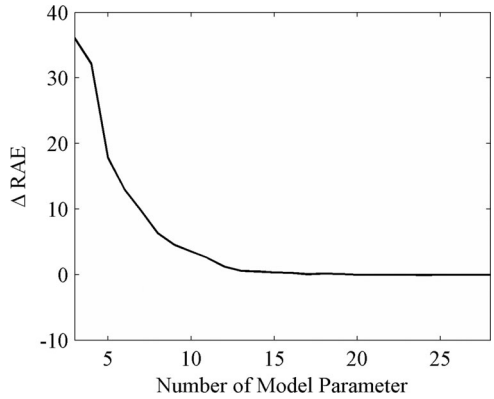

Fig. 8. Relative absolute error versus model parameters of the identification model.

From Table V, it can be seen that the response of Model 1 and 2 is similar. However, the reduced model contains fewer parameters, which is important for real-time implementation.

In the second and the third scenario, the response of the control system when there are uncertainties or unmodeled dynamics between the identification model and the prototype is studied. Table VI shows the results for the second prototype. In this case, the control based on Model 2 performs slightly better than when Model 1 is used for model-based control. The RMS using Model 2 is 10% lower than in Model 1.

Table VII shows the results for the third scenario. As in the second scenario, the control systems based on Model 2 perform better than those based on Model 1. The RMS of Model 2 is 18% lower than Model 1.

D. Discussion

The results presented in this section indicate that the control system based on the set of relevant parameters performs better when compared with the identified model containing all the parameters contributing to the robot dynamic (Model 1). This occurs for two reasons. The first one can be concluded from Fig. 8, which presents the relative value of the relative absolute error (ERA) as a function of the number of model parameters. It can be seen that the era between models containing 12 and 28 parameters are similar. The differences among the models are of less than 1%. These 16 parameters make a poor contribution to the dynamic systems response, which imply that the regression

TABLE VIII
IDENTIFIED RELEVANT PARAMETERS FOR THE ACTUAL ROBOT, SI UNITS

Parameter	$\vec{\Phi}^r$	σ^r
$my_3 - \sin(2\pi/3)\, l_m \cdot \sum_{i=1}^{5} m_i$	-16.32	1.96
$\sum_{i=1}^{7} m_i$	53.96	1.55
$Izz_7 + l_r^2 \cdot \sum_{i=1}^{5} m_i$	45.99	11.58

matrix is ill-conditioned. Models above 12 parameters have infeasible parameters, so these models are meaningless. On the other hand, the parameters from the complete model have a strong near-dependence between the columns of the regression matrix. This linear near-dependence is demonstrated via regression of any column of W on all the others columns. For instance, regressing the column of Parameter 5 of Table I with respect to the columns of the reduce model leads to a correlation of about 80%. Thus, some of the contribution of the parameter is identified when using the Model 2.

It is important to highlight that the reduced model is identified with physically feasible dynamic parameters. This is very important aspect in advanced model control where the mass matrix $\mathbf{M}$ must be positive definite to avoid problems when inverting the matrix, for instance [30]. On the other hand, the reduced model gives a good prior knowledge of the parallel robot, thus dynamics coupling effects can be reduced when developing the control system.

V. MODEL-BASED CONTROL FOR THE ACTUAL PM

Experiments were conducted over the actual parallel robot. As has previously been mentioned, the robot has three legs. The linear movement in prismatic joints is provided by BMS465 dc brushless motors via a ball screw mechanism. The dc motors with their built-in rotary encoders and linear guides are fixed to the base platform. The displacement in the prismatic joint is related to the encoders by the pitch of the ball screw. The tracking control is performed using the values from the encoders. The control algorithms were implemented on a 2.05 GHz Intel Core 2 Quad/Duo processor equipped with Advantech data acquisition cards. Aerotech BA10 amplifiers were used to provide control actions. The control algorithms were developed in a Visual C++ environment.

Six different trajectories were used for identification. These trajectories are different from the test trajectories. In Table VIII, the mean and percentage deviation for rigid body dynamic parameters of the 3-PRS PM for the reduced model are listed. As can be seen from Table VIII, the values of the parameters are feasible, for instance: $\sum_{i=1}^{7} m_i > 0$. This set of parameters is used for designing passivity-based control.

The control gains of this controller were tuned and determined with experiments, $\mathbf{K}_p = 250, \mathbf{K}_d = 25$. After that, the four test trajectories used in simulations are implemented on the actual robot. Table IX shows the RMS error from experiments. As was expected from the results and discussion in the simulation performed, errors for the reduced model (Model 2) are lower than those obtained for the complete model (Model 1).

TABLE IX
ROOT MEAN SQUARE FOR THE ACTUAL ROBOT

Trajectory (ε_{RMS}) [mm]	1	2	3	4
Model 1	0.8679	1.4869	1.2938	1.5737
Model 2	0.5026	0.6211	0.4935	0.5379

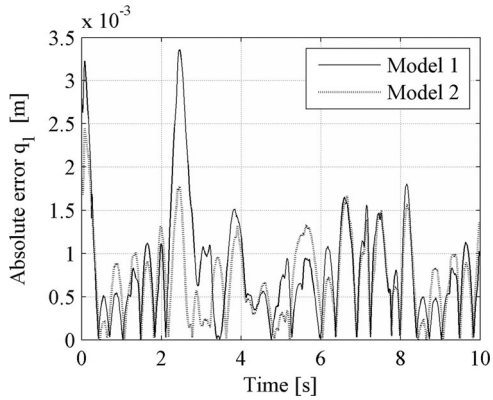

Fig. 9. Joint absolute error in one of the actuator for a test trajectory.

Fig. 9 shows the joint absolute error for one of the test trajectories followed. It can be seen that the model-based control that used the reduced model outperforms the one that used the complete model.

Further test indicates that the model-based control based on the reduced model is able to obtain tracking path errors within 2×10^{-3} m. On the other hand, when the complete model is used, the path error is within 3.5×10^{-3}.

VI. CONCLUSION

In this paper, two dynamic models for developing model-based control of a 3-DOF PM were considered. The complete model contains all the dynamic parameters affecting the dynamic behavior of the robot. The reduced model contains only a set of relevant parameters obtained through a process which considers the robot's leg symmetries, the statistical significance of the identified parameters, and the physical feasibility of the parameters. A virtual and an actual prototype of the parallel robot were built. The virtual prototype allowed testing of the robot tracking position performance by using passivity-based controllers. Three different scenarios based on the differences between the virtual prototype and the identification models were considered. The test trajectories were designed to cover the operative capabilities of the PM. The results indicate that the reduced model perform better than the complete one. After that, the same procedure was followed with the actual PM. Findings show that when the relevant parameters are used, the level of error is significantly lower than when the complete model is considered. Moreover, the use of the reduced model not only required a lower computational load than the complete model, but it is also able to generate very good tracking performance.

REFERENCES

[1] I. Theodor, "Standardization of terminology," *Mech. Mach. Theory*, vol. 38, no. 7–10, pp. 597–1111, 2003.

[2] F. Pierrot, V. Nabat, O. Company, S. Krut, and P. Poignet, "Optimal design of a 4-DOF parallel manipulator: From academia to industry," *IEEE Trans. Robot.*, vol. 25, no. 2, pp. 213–224, Apr. 2009.

[3] O. Bebek, M. J. Hwang, and M. C. Cavusoglu, "Design of a parallel robot for needle-based interventions on small animals," *IEEE/ASME Trans. Mechatronics*, to be published.

[4] W. Khalil and E. Dombre, *Modeling Identification and Control of Robots*. London, U.K.: Hermes Penton, 2002.

[5] D. Kim, J. Y. Kang, and K. I. Lee, "Nonlinear robust control design for a 6-DOF parallel robot," *KSME Int. J.*, vol. 13, no. 7, pp. 557–568, 1999.

[6] K. Fu and J. K. Mills, "Robust control design for a planar parallel robot," *Int. J. Robot. Autom.*, vol. 22, no. 2, pp. 139–147, 2007.

[7] S. D. Stan, R. Balan, V. Maties, and C. Rad, "Kinematics and fuzzy control of ISOGLDE3 medical parallel robot," *Mechanika*, vol. 1, no. 75, pp. 62–66, 2009.

[8] H. B. Gou, Y. G. Liu, G. R. Liu, and H. R. Li, "Cascade control of a hydraulically driven 6-dof parallel robot manipulator based on a sliding mode," *Control Eng. Pract.*, vol. 16, no. 9, pp. 105–1068, 2009.

[9] H. Abdellatif and B. Heimann, "Advanced model-based control of a 6-DOF hexapod robot: A case study," *IEEE/ASME Trans. Mechatronics*, vol. 15, no. 2, pp. 269–279, Apr. 2010.

[10] A. Codourey, "Dynamic modeling of parallel robots for computed-torque control implementation," *Int. J. Robot. Res.*, vol. 17, no. 12, pp. 1325–1336, 1998.

[11] Q. Li and F. X. Wu, "Control performance improvement of a parallel robot via the design for control approach," *Mechatronics*, vol. 14, no. 8, pp. 947–964, 2004.

[12] Y. Li and Q. Xu, "Dynamic modeling and robust control of a 3-PRC translational parallel kinematic machine," *Robot. Comput.-Integr. Manuf.*, vol. 25, no. 3, pp. 630–640, 2009.

[13] P. Renaud, A. Vivas, N. Andreff, P. Poignet, F. Pierrot, and O. Company, "Kinematic and dynamic identification of parallel mechanisms," *Control Eng. Pract.*, vol. 14, no. 9, pp. 1099–1109, 2006.

[14] Y. X. Zhang, S. Cong, W. W. Shang, Z. X. Li, and J. S. Long, "Modeling, identification and control of a redundant planar 2-dof parallel manipulator," *Int. J. Control, Autom. Syst.*, vol. 5, no. 5, pp. 559–569, 2007.

[15] N. Farhat, V. Mata, ÁA. Page, and F. Valero, "Identification of dynamic parameters of a 3-DOF RPS parallel manipulator," *Mech. Mach. Theory*, vol. 43, no. 1, pp. 1–17, 2008.

[16] H. Abdellatif and B. Heimann, "Experimental identification of the dynamics model for 6-DOF parallel manipulators," *Robotica*, vol. 28, no. 03, pp. 359–368, 2010.

[17] W. W. Shang, S. Cong, and F. R. Kong, "Identification of dynamic and friction parameters of a parallel manipulator with actuation redundancy," *Mechatronics*, vol. 20, no. 2, pp. 192–200, 2010.

[18] M. Díaz-Rodríguez, V. Mata, N. Farhat, and S. Provenzano, "Identifiability of the dynamic parameters of a class of parallel robots in the presence of measurement noise and modeling discrepancy," *Mech. Based Des. Struct. Mach.*, vol. 36, no. 4, pp. 478–498, 2008.

[19] C. M. Pham and M. Gautier, "Essential parameters of robots," in *Proc. 30th IEEE Conf. Decis. Control*, Dec. 1991, pp. 2769–2774.

[20] G. Antonelli, F. Caccavale, and P. Chiacchio, "A systematic procedure for the identification of dynamic parameters of robot manipulators," *Robotica*, vol. 17, no. 4, pp. 427–435, 1999.

[21] K. Yoshida and W. Khalil, "Verification of the positive definiteness of the inertial matrix of manipulators using base inertia parameters," *Int. J. Robot. Res.*, vol. 49, no. 5, pp. 498–510, 2000.

[22] H. Olsson, K. J. Åström, C. Canudas-de Wit, and M. Gäfvert, P. Lischinsky, "Friction models and friction compensation," *Eur. J. Control*, vol. 4, no. 3, pp. 176–195, 1998.

[23] R. Wehage and E. Haug, "Generalized coordinates partitioning for dimension reduction in analysis of constrained dynamic system," *ASME J. Mech. Des.*, vol. 104, no. 1, pp. 247–255, 1982.

[24] M. Gautier, "Numerical calculation of the base inertial parameters of robots," *J. Robot. Syst.*, vol. 8, no. 4, pp. 485–506, 1991.

[25] M. Díaz-Rodríguez, V. Mata, A. Valera, and A. Page, "A methodology for dynamic parameters identification of 3-DOF parallel robots in terms of relevant parameters," *Mech. Mach. Theory*, vol. 45, no. 9, pp. 1337–1356, 2010.

[26] R. Ortega and M. Spong, "Adaptive motion control of rigid robots: A tutorial," *Automatica*, vol. 10, no. 5, pp. 561–577, 1989.

[27] M. W. Walker and D. Orin, "Efficient dynamic computer simulation of robotic mechanisms," *J. Dyn. Syst., Meas. Control*, vol. 104, pp. 205–211, 1982.

[28] B. Paden and R. Panja, "Globally asymptotically stable PD+ controller for robot manipulators," *Int. J. Control*, vol. 47, no. 6, pp. 1697–1712, 1988.

[29] J. Swevers, C. Ganseman, J. DeSchutter, and H. VanBrussel, "Experimental robot identification using optimised periodic trajectories," *Mech. Syst. Signal Process.*, vol. 10, no. 5, pp. 561–577, 1996.

[30] C. F. Yang, J. W. Han, and Q. T. Huang, "Decoupling control for spatial six-degree-of-freedom electro-hydraulic parallel robot," *Robot. Comp-Integr. Manuf.*, vol. 28, no. 1, pp. 14–24, 2012.

[31] H. S. Kim, Y. M. Cho, and K. I. Lee, "Robust nonlinear task space control for 6 DOF parallel manipulator," *Automatica*, vol. 41, no. 9, pp. 1591–1600, 2005.

Miguel Díaz-Rodríguez received the Engineer degree in mechanical engineering and the M.Sc. degree in applied engineering mathematics from the Universidad de los Andes, Mérida, Venezuela, in 2000 and 2005, respectively, and the Doctor degree in mechanical engineering from the Universidad Politécnica de Valencia, Valencia, Spain, in 2009.

Since 2011, he has been an Associate Professor in the School of Mechanical Engineering, Universidad de los Andes. His research activities include robot kinematics, robot dynamics, design of parallel robots, dynamic parameter identification, and biomechanics.

Angel Valera received the B.Eng. degree in computer science, in 1988, the M.Sc. degree in computer science, in 1990, and the Ph.D. degree in control engineering, in 1998, all from the Universidad Politécnica de Valencia (UPV), Valencia, Spain.

He has been a Professor of automatic control at the UPV since 1989, and currently he is a Full Professor in the Department of Systems Engineering and Control. He has taken part in research and mobility projects funded by local industries, government, and the European community, and he has authored/coauthored more than 140 technical papers in journals, technical conferences, and seminars. His research interests include industrial and mobile robot control and mechatronics.

Vicente Mata received the Engineer and Ph.D. degrees in mechanical engineering from the Universidad Politécnica de Valencia (UPV), Valencia, Spain, in 1978 and 1985, respectively.

Since 2002, has been a Full Professor in the Department of Mechanical Engineering, UPV. His research activities include robot path planning, robot dynamics, design of parallel robots, dynamic parameter identification, and biomechanics.

Marina Vallés received the degree in computer science and the M.Sc. degree in CAD/CAM/CIM from the Universidad Politécnica de Valencia (UPV), Valencia, Spain, in 1996 and 1997, respectively.

Since 1999, she has been a Lecturer in the Department of Systems Engineering and Control, UPV. She currently teaches courses on automatic control and computer simulation. Her research interests include real-time systems, automatic code generation, and control education.